Materials Sciences Research Journal 2008, Volume 2, Issue 3/4 ISSN 1935-2441
pp.241-258

GAS PRESSURE FORMING OF SPHERICAL DOMES FROM PB-SN EUTECTIC ALLOY SUPERPLASTIC SHEET MATERIAL

***J. J. V. Jeyasingh*[a], *B. Nageswara Rao*[*,b], and *A. Chennakesava Reddy*[c]**

[a]Mechanical Engineering Entity, Vikram Sarabhai Space Centre,
Trivandrum-695 022, India
[b]Structural Analysis and Testing Group, Vikram Sarabhai Space Centre,
Trivandrum-695 022, India
[c]Faculty of Mechanical Engineering, JNTU College of Engineering,
Ananthapur-515 002, India

ABSTRACT

Gas pressure bulging of metal sheets has become an important forming method. As the bulging process progresses, significant thinning in the sheet material becomes inevitable. A prior knowledge about non-uniform thinning in the product after forming helps the designer in the selection of initial blank thickness. This paper presents a simple analytical procedure on the thinning of superplastically formed Pb-Sn eutectic alloy spherical domes. It also addresses the issue of instability of deformation.

Keywords: Superplastic deformation; bulge forming; fracture strain.

1. INTRODUCTION

Superplastic forming (SPF) has a wide application in the aviation and aerospace industries since it is of great advantage in the manufacture of very complicated, light and strong components [1-3]. Superplasticity has been observed in metals (including aluminium, magnesium, iron, titanium and nickel-based alloys), ceramics (including monoliths and composites), intermetallics (including iron, nickel, and titanium base) and laminates. Chokalingam et al. [4] have conducted experiments on Pb-Sn eutectic alloy sheet at room

* Corresponding author, E-mail: bnrao52@rediffmail.com; Phone No: + 91 471 2565831; Fax No. + 91 471 2564181

temperature. Dutta and Sharma [5] have presented a rigorous mathematical analysis to predict the thickness variation at any point of a hemisphere after forming. There are two main types of superplastic behavior: micrograin or microstructural superplasticity, and transformation or environmental superplasticity. By thermally cycling through their transformation temperature range, coarse-grained, polymorphic materials can be deformed superplastically, owing to the emergence of transformation mismatch plasticity (or transformation superplasticity) as a deformation mechanism [6,7]. Khraisheh [8] has examined the failure characteristics of superplastic sheet materials under gas pressure forming. Wu [9] has performed a series of experiments using various strain rates and strain states during the superplastic deformation of a fine-grained 8090 aluminum alloy. Tong and Chan [10] have examined the deformation behavior of a high-strain-rate superplastic (HSRS) Al-4.4Cu-1.5Mg/21SiC$_w$ sheet under uniaxial and equibiaxial tension. It is noted that the flow stress-strain rate relationship determined from uniaxial tension can be used for forming processes subject to complex stress states. The amount of cavity increases with increasing strain. The amount of cavity obtained under equibiaxial tension is slightly larger than that under uniaxial tension at the same effective strain rate. Chan and Tong [11] have investigated the cavitation behavior and forming limits for the superplastic material under biaxial tension. Dutta [12] has presented a mathematical analysis and validated by blowing a profiled blank to a dome of nearly uniform thickness profile. Chung et al. [13] have provided a detailed description of superplastic behavior of the AZ61 magnesium alloy sheet under conditions of biaxial tensile deformation. Chan and Tong [14] have examined the deformation and cavitation behavior of a HSRS 21 vol% SiC whisker-reinforced Al-4.4Cu-1.5Mg under biaxial stress states with variable strain rate paths. Xing et al. [15] have proposed a pre-form design method for sheet superplastic bulging with finite element modeling. Yoon et al. [16] have presented the optimization of thickness distribution of diffusion bonded initial blank and the prediction of the thickness at final forming stage for a spherical titanium tank. The necessary requirements to achieve superplasticity are: fine and equiaxed grain size (<10μm); forming temperature (>0.5Tm) and controlled strain rate.

SPF is a near net-shape forming process which offers many advantages over conventional forming operations including low forming pressure due to low flow stress, lower die cost, greater design flexibility, and the ability to shape hard metals and form complex shapes. However, the widespread use of SPF has been hampered by a number of issues including limited predictive capabilities of deformation and fracture [17-27]. Wu [18] has investigated the cavitation behavior of a superplastic 8090Al alloy during equi-biaxial tensile deformation. In order to unify the thickness and to decrease the cavity, the thickness distribution of sheet was controlled by using the rotary forging [19]. Chung and Cheng [21] have proposed a fracture criterion in terms of the flow localization factor for superplastic materials that are not sensitive to cavity growth. Carrino et al. [23] have examined the cavity growth rate of pre-machined voids on Pb-Sn alloy specimens subject to the tensile deformation and to the biaxial deformation. The void growth increases for the low values of the strain rate sensitivity and the strain hardening index in the biaxial deformation. Kalaichelvan et al. [24] have made cavity minimization and uniformity on superplastic forming of thin eutectic Pb-Sn sheet through optimum loading and pre-forming. Nozzal et al. [27] have examined the effects of strain rate sensitivity variation on the stability of deformation during superplastic forming. There is a need to develop accurate models that can predict the deformation and failure behavior of superplastic materials.

The bulge forming of domes is usually involved in the early stages of commercial forming process and has attracted the attention of many investigations. Their interest has been concentrated on the investigation of the dome height-time relationship and the thickness distribution along the dome profile. The variation of thickness has been found to be an important feature of this process. Figure 1 shows a schematic diagram of the setup using gas pressure forming. The top chamber holds the gas (air) at the predetermined pressure profiles through a pressure control system. The openings of the valves are adjusted through a proper closed-loop control scheme. The bottom die contains a cavity which configures same as the component. Using suitable spacers and fixtures, the top and bottom chambers will be mounted coaxially onto the platen of a hydraulic press to apply loads for holding the blank during the forming operation.

Spherical bulge forming is always used as a fundamental study of the superplastic formability. It involves many mechanical and geometrical features such as damage evolution, ductility variation, strength level, thickness distribution, etc. In mechanical modeling of superplastic deformation, the material is assumed to obey von Mises' effective stress and strain criteria [29-33]. Unlike aluminium and titanium alloys, the Pb-Sn alloy exhibits good superplasticity even at room temperature [34, 35].

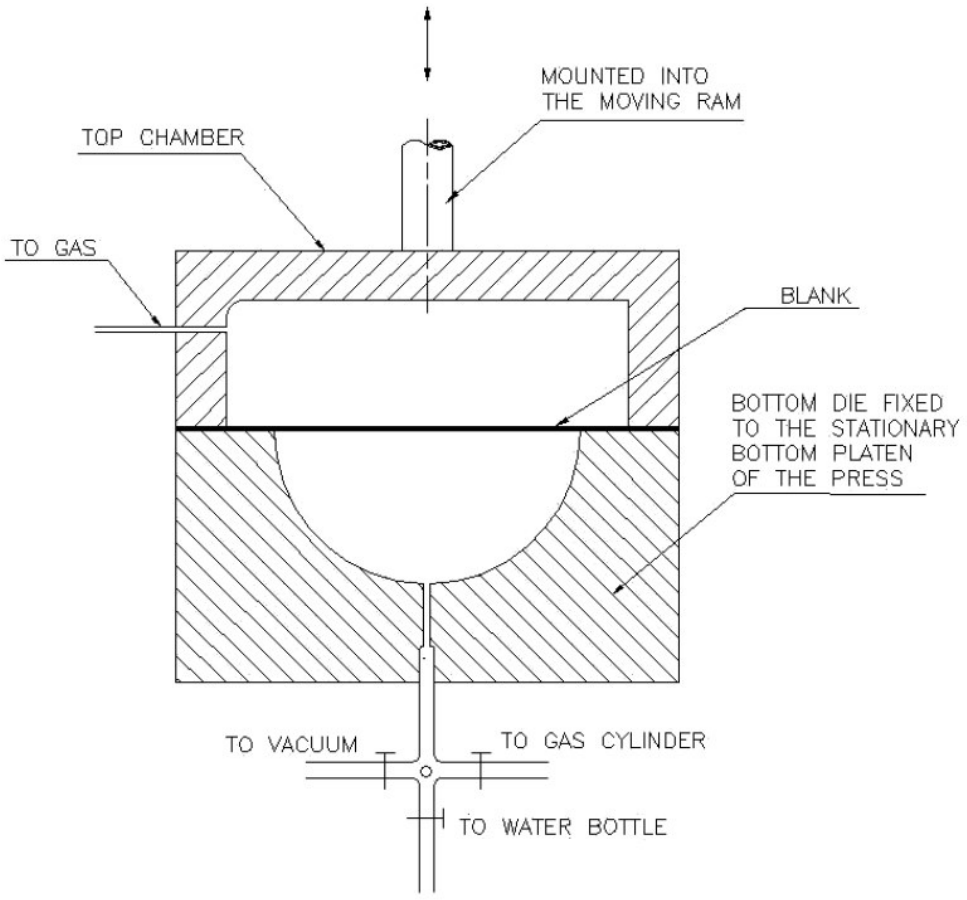

Figure 1. Schematic diagram of the setup using gas pressure forming.

This material characteristic minimizes the experimental costs, as the aluminium and titanium alloys require high-forming temperatures. Chokalingam et al. [4], Khraisheh [8, 17], Huang et al. [20], Kalaichelvan et al. [24], Giuliano et al. [26], and Jeyasingh et al. [36,37] have made studies on the Pb-Sn eutectic alloy. Uniaxial tests on the superplastic Pb-Sn eutectic alloy (Sn-38.1%Pb alloy) showed appreciable grain shape changes and distortion [8]. While forming superplastic Pb-Sn eutectic alloy sheet material at an effective constant strain rate, Khraisheh [8] observed that failure occurred at the pole of the dome. The forming time at failure was found to be close to the peak value of the forming pressure profile. The instability analysis of Khraisheh [8] could not estimate accurately the limiting thickness strains at the pole of the spherical dome. However, these experimental investigations on the Pb-Sn superplastic alloy are useful to SPF industry in developing general guidelines and procedures. This paper examines the instability of deformation during gas pressure forming of superplastic Pb-Sn eutectic alloy sheet material.

2. ANALYSIS

Thermo-mechanical constitutive equations of superplastic materials describe the relationship between the flow stress (σ), strain (ε), strain rate ($\dot{\varepsilon}$), temperature (T) and other microstructural quantities, usually the grain size (d). The mathematical relationship employs a number of model / material parameters (co-efficients) and material constants. Based on the phenomenological form of superplastic behaviour, the uniaxial flow stress σ is found to be a strong function of inelastic strain-rate $\dot{\varepsilon}$ and a weak function of strain ε and grain size d. A functional form of the constitutive relationship is given by [38]

$$\sigma = K\left(\dot{\varepsilon}\right)^m, \tag{1}$$

where K and m are material constants. 'm' in Eq. (1) is known as the strain-rate sensitivity index of the material. Eq. (1) indicates that the flow stress is governed by the strain rate sensitivity m, which is a function of the material properties. For superplastic behavior, m needs to be greater than or equal to 0.3 with the majority of superplastic materials having an m that lies in the range 0.4-0.8. The value of m varies with strain rate and needs to be held at a maximum "optimum" value during forming. This is usually achieved by defining a blow pressure profile to optimize the strain rate.

In the mechanical modeling of superplastic deformation, the material is assumed to be purely inelastic and incompressible. The diaphragm is rigidly clamped at the periphery. The bulge surface shape keeps to that of a part of a sphere (see Figure 2). The thickness (s) of the specimen is very small compared with the die radius (a). The radial stress (σ_r) in the thickness direction is usually very small compared to the meridional stress (σ_m) or the hoop stress (σ_θ). The stress state in the dome is: $\sigma_m > 0$, $\sigma_\theta > 0$, $\sigma_r \approx 0$. A balanced biaxial stress state (i.e., $\sigma_m = \sigma_\theta$) exists at the dome apex. At the edge of the dome, there is a constraint around the periphery, leading to a plane-strain stress state. Therefore, the stress gradient in a forming dome causes a more rapid thinning rate at the pole, and it may be expected that the

thinning difference will accelerate with time, leading to a thickness gradient in the formed dome.

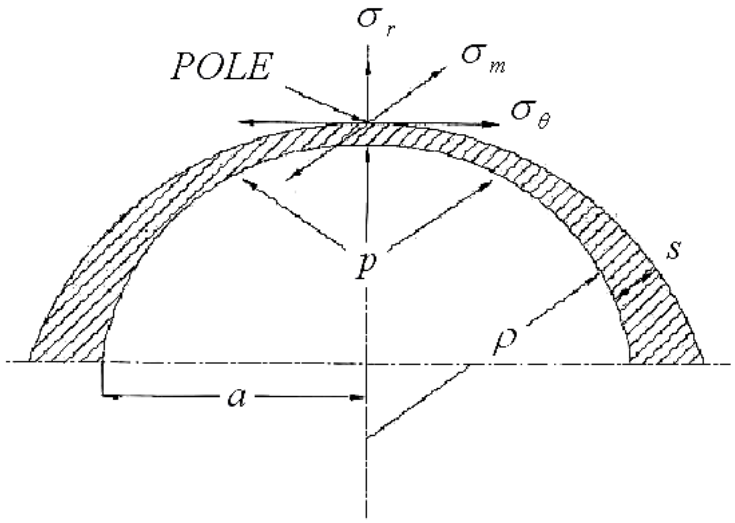

Figure 2. Schematic representation of formed dome.

Assuming plane stress and balanced biaxial stretching at the pole of the dome, one can write:

$$\sigma_r = 0, \sigma_\theta = \sigma_m = \frac{P\rho}{2s},\ \sigma_e = \sigma_\theta \tag{2}$$

$$\varepsilon_\theta = \varepsilon_m, \varepsilon_\theta + \varepsilon_m + \varepsilon_r = 0,\ \varepsilon_e = -\varepsilon_r \tag{3}$$

where P is the forming pressure; ρ is the radius of curvature; σ_e is the von Mises effective stress; and ε_e is the effective strain. Thickness strain (ε_r) is compressive in nature whereas the effective strain (ε_e) is positive.

Let M be some point on the membrane, which at the initial moment of time (t = 0) belongs to the diameter AB (see Figure 3). The envelope is clamped around its periphery and r_0 is the distance between point M and the centre of membrane O. At some current moment of time t > 0, point M goes to M′, while point O goes to point O′.

The hoop, meridional and thickness strains at M′ are:

$$\varepsilon_\theta = \ell n\left(\frac{\rho\alpha}{a}\right) \tag{4}$$

$$\varepsilon_m = \ell n\left(\frac{2\pi r}{2\pi r_0}\right) = \ell n\left(\frac{\rho\alpha}{a}\frac{\sin\phi}{\phi}\right) \tag{5}$$

$$\varepsilon_r = \ell n\left(\frac{s_\phi}{s_0}\right) \tag{6}$$

where s_ϕ is the thickness at M′. α is the half angle subtended by the dome surface at its centre of curvature and ϕ is the angle between the symmetry axis and the dome radius, drawing to the point under consideration.

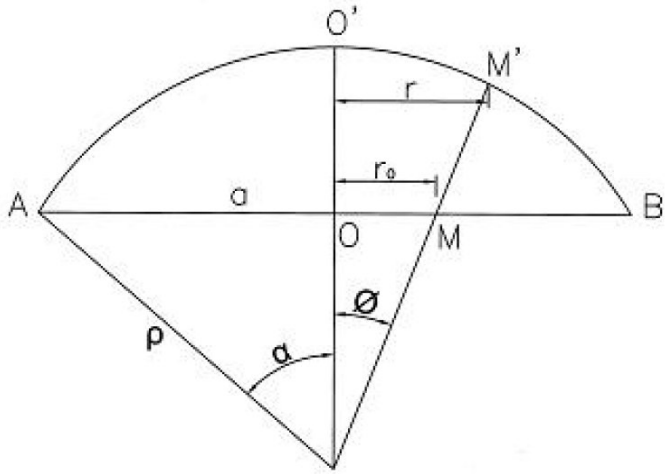

Figure 3. Schematic representation of bulge forming of sheets.

Using Eqs. (4)-(6) in Eq. (3), s_ϕ can be expressed in the form

$$\frac{s_\phi}{s_0} = \left(\frac{\sin\alpha}{\alpha}\right)^2 \frac{\phi}{\sin\phi} \tag{7}$$

An empirical relation for the spherical dome thickness (s_ϕ) is [31]:

$$s_\phi = s_p + \left(s_e - s_p\right)\left(\frac{\phi}{\alpha}\right)^2 \tag{8}$$

Here s_p is the thickness at the pole of the dome. The thickness at the edge of the dome (s_e) is:

$$s_e = \left[\left(1-C\right)s_0^{\frac{1}{m}} + Cs_p^{\frac{1}{m}}\right]^m \tag{9}$$

where $C = \left(\frac{\sqrt{3}}{2} \right)^{1+\frac{1}{m}}$

Assuming volume constancy, one can write

$$\pi a^2 s_0 = 2\pi \rho^2 \int_0^{\alpha} s \sin\phi \, d\phi \tag{10}$$

Using Eq. (8) in Eq. (10), one can obtain

$$s_0 = 2 \cos ec^2 \alpha \left[s_p I_0 + (s_e - s_p) I_1 \right] \tag{11}$$

where $\rho = a \cos ec \alpha$, $I_0 = 1 - \cos\alpha$ and $I_1 = -\cos\alpha + \frac{2\sin\alpha}{\alpha} - \left(\frac{2}{\alpha} \sin\frac{\alpha}{2} \right)^2$

Using Eq. (9) in Eq. (11), one can obtain a non-linear equation to s_p. For the specified '*m*', the thickness at the pole (s_p) can be determined by solving the resulting non-linear equation through Newton Raphson's iterative method.

3. RESULTS AND DISCUSSION

After solving Eq. (11), the thickness at the pole of the dome (s_p) is expressed in the form:

$$\frac{s_p}{s_0} = \left(\frac{\sin\alpha}{\alpha} \right)^2 \left\{ 1 + a_1\alpha + a_2\alpha^2 + a_3\alpha^3 + a_4\alpha^4 \right\} \tag{12}$$

Table 1 gives the values of a_1, a_2, a_3 and a_4 for the specified strain rate sensitivity index (*m*).

Chokalingam et al. [4] have conducted experiments on Pb-Sn eutectic alloy sheet at room temperature. The diameter and thickness of the sheet are 220 mm and 1.3 mm respectively. The strain rate sensitivity index (*m*) of the sheet material is 0.4. The die diameter is 80 mm. The blank is subjected to an air pressure of 0.2 MPa. From Eqs. (9) and (12), the thicknesses at the pole and equator of the spherical dome obtained are: s_p = 0.402 mm and s_e = 0.926 mm against the measured values of 0.36 and 0.92 respectively.

Dutta and Sharma [5] presented the optimum temperature, strain rate, flow-stress and strain-rate sensitivity for the titanium alloy (Ti-6.3Al-2.7Mo-1.7Zr) were: 1173 K, 3.3 x $10^{-4}s^{-1}$, 7.06 MPa and 0.85. It is noted from their experimental results that a hemisphere of diameter

30.3 mm was formed, by blowing a 2.7 mm thick blank by argon gas. The pole thickness obtained from Eq. (12) is 1.145 mm, which is close to the measured thickness of 1.194 mm.

Table 1. Values of a_1, a_2, a_3 and a_4 in Eq. (12) for the specified strain rate sensitivity index (m)

Strain rate sensitivity index (m)	Constants in equation (12)			
	a_1	a_2	a_3	a_4
0.20	0.0023	-0.0396	0.0638	-0.1249
0.25	0.0179	-0.1095	0.1987	-0.1692
0.30	0.034	-0.1741	0.2967	-0.192
0.35	0.0388	-0.1843	0.3110	-0.1824
0.40	0.0352	-0.1582	0.2749	-0.1558
0.45	0.0301	-0.1253	0.2295	-0.1284
0.50	0.0247	-0.0945	0.1883	-0.1053
0.55	0.0202	-0.0681	0.1529	-0.0860
0.60	0.0169	-0.0485	0.1271	-0.0718
0.65	0.0134	-0.0299	0.1035	-0.0595
0.70	0.0117	-0.0190	0.0895	-0.0513
0.75	0.0096	-0.0075	0.0754	-0.0438
0.80	0.0086	-0.0003	0.0662	-0.0384
0.85	0.0075	0.0067	0.0575	-0.0336
0.90	0.0067	0.0119	0.0513	-0.0299
0.95	0.0059	0.0166	0.0458	-0.0268
1.00	0.0055	0.0196	0.0425	-0.0245

3.1. Generation of Forming Pressure – Time Curve

SPF is highly sensitive to strain rate. Thus it is essential to generate an accurate pressure-time profile to maintain the desired strain rate, during deformation. Dutta and Mukherjee [29] derived a relationship based on biaxial stress conditions to maintain a constant strain rate during superplastic blow forming of a hemisphere. Thickness variation along the dome profile occurring during the deformation was not taken into account, which results overestimation on the pole thickness and the forming pressure. A simple and accurate procedure on the generation of forming pressure-time curve is described below by taking into account the thickness variation along the dome profile occurring during the deformation.

From Eqs. (3) and (6), the thickness at the pole (s_p) at a given forming time (t) under an effective constant strain rate ($\dot{\varepsilon}_e$) can be obtained from:

$$s_p = s_0 \exp\left(-\dot{\varepsilon}_e t\right) \tag{13}$$

From Eqs. (1) and (2), one can express the forming pressure (P) in the form

$$P = \frac{2\sigma_e s_p}{\rho} = \frac{2K\dot{\varepsilon}^m s_p}{\rho} = \frac{2K\dot{\varepsilon}^m s_0}{a} \sin\alpha \left(\frac{s_p}{s_0}\right) \tag{14}$$

and the forming time (t) from Eq. (13) is

$$t = \frac{1}{\dot{\varepsilon}} \ln\left(\frac{s_0}{s_p}\right) \tag{15}$$

The basic inputs for generation of pressure-time curve are: the initial blank thickness (s_0), die radius (a) and the applied strain rate ($\dot{\varepsilon}_0$). For the spherical dome formation, α varies between 0 and $\frac{\pi}{2}$. For each value of α, the pole thickness s_p is obtained from Eq. (12). Specifying α and s_p in Eqs. (14) and (15), one can obtain the pressure (P) and the corresponding forming time (t).

3.2. Dome Height with Forming Time under Applied Pressure

Using Eqs. (1), (2) and (12), one can derive the following differential equation to obtain α with the forming time, t for the applied pressure (P):

$$\frac{d\alpha}{dt} = -\frac{1}{2}\left(\frac{Pa}{2Ks_0}\right)^{\frac{1}{m}} F(\alpha) \tag{16}$$

where

$$F(\alpha) = \left(\frac{\alpha^2}{f(\alpha)\sin^3\alpha}\right)^{\frac{1}{m}} \frac{\alpha \sin\alpha f(\alpha)}{\left\{(\alpha\cos\alpha - \sin\alpha) f(\alpha) + \frac{1}{2}\alpha \sin\alpha f'(\alpha)\right\}}, \tag{17}$$

$$f(\alpha) = 1 + a_1\alpha + a_2\alpha^2 + a_3\alpha^3 + a_4\alpha^4, \tag{18}$$

and prime denotes differentiation with respect to α.

Initial condition for Eq. (16):

$\alpha = 0$ at $t = 0$ (19)

For a very small forming time, Eqs. (16) and (19) give

$$\alpha = \left[\frac{Pa}{2Ks_0} \left\{ \frac{3}{2} \left(2 + \frac{1}{m} \right) t \right\}^m \right]^{\frac{1}{1+2m}} \tag{20}$$

The height of the dome (h) from the solution of α is:

$$h = \frac{a}{\sin \alpha} (1 - \cos \alpha) \tag{21}$$

Specifying the values of ϕ between 0 and α, the thinning of the dome can be obtained from Eqs. (8), (9) and (12). The von Mises' equivalent strain at the pole of the dome is obtained from

$$\varepsilon_e = -\varepsilon_r = \ell n \left(\frac{s_o}{s_p} \right) \tag{22}$$

Frary et al. [7] have investigated under biaxial stress conditions during thermal cycling of titanium alloys and composites. They used the CHIP process, which consists of blending of elemental metallic powders, cold isostatic pressing, vacuum sintering, and finally container less hot isostatic pressing to fabricate Commercial – Purity titanium (CP-Ti) and Ti-6Al-4V with and without discontinuous reinforcements. TiC particles (in the amount of 10 vol %) were added to both CP-Ti and Ti-6Al-4V. These composites referred as Ti/TiC_p and Ti-6Al-4V/TiC_p. Ti-6Al-4V reinforced with 5 vol % TiB whiskers and referred the composite as Ti-6Al-4V / TiB_w Disks of each material were machined from near-net-shape densified plates, with density greater than 99%. The disks had a diameter of 62 mm and a thickness ranging from 1.36 to 1.59 mm. The disk specimens were clamped into an Inconel pressurization vessel with an open die radius of 24 mm. Experiments were performed under gas pressure of 0.2 MPa and over the temperature range (840 to 970 ^{o} C) of the thermal cycle (frequencies: 15 h^{-1} for CP-Ti and 7.5 h^{-1} for Ti-6Al-4V and the respective composites). From the biaxial experiments of Frary et al. [7] for titanium alloys and composites, the constitutive relation is

$$\dot{\varepsilon} = K_{TSP} \sigma \tag{23}$$

Here K_{TSP} is a constant for the transformation superplasticity. The strain rate sensitivity index (m) is found to be unity. From Eq. (23), one can express the material constants in Eq. (1) as: m=1 and $K = \frac{1}{K_{TSP}}$. Table-2 gives a good comparison of analytical and experimental results related to the pole thickness of the domes made of titanium alloys and composites. In the present analysis, Eq. (16) is solved by the finite difference method with a fixed step-size,

Δt = 100 seconds. Figures 4 and 5 show the comparison of analytical and experimental results of dome height (h) with respect to the forming time for titanium alloy (Ti-6Al-4V) and titanium matrix composite (Ti-6Al-4V/TiC_p). The analytical results are found to be reasonably in good agreement with test results.

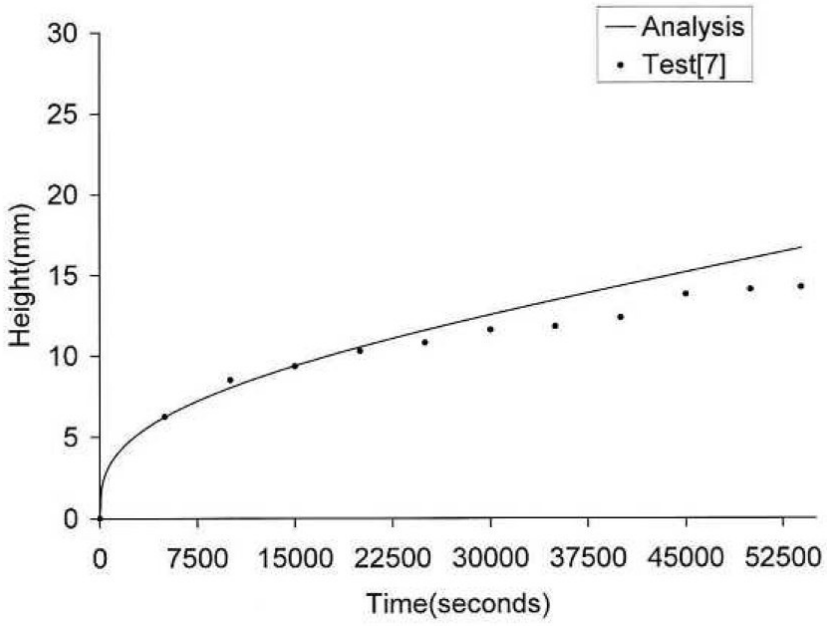

Figure 4. Variation of dome height with time for titanium alloy, Ti-6Al-4V.

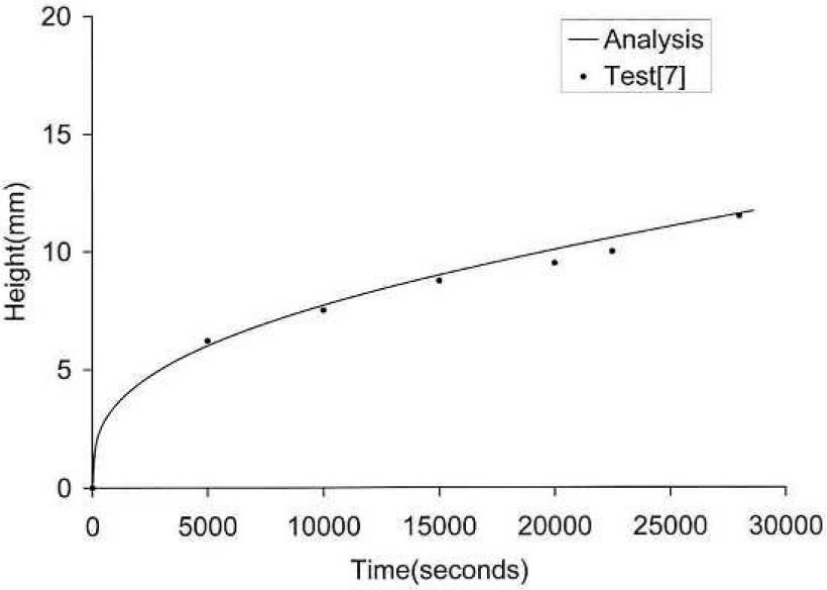

Figure 5. Variation of dome height with time for titanium matrix composite, Ti-6Al-4V/TiC_p.

Table 2. Comparison of analytical and experimental pole thickness of spherical domes made of titanium alloys and composites after superplastic forming

Material	Test [7]				Present Analysis		
	K_{TSP} x 10^{-12}Pa^{-1}s^{-1}	s_0 (mm)	s_p (mm)	ε_e Eq.(20)	α (degrees)	s_p (mm)	ε_e Eq.(20)
CP-Ti	9.58	1.390	0.636	0.782	87.50	0.638	0.779
Ti/TiC$_p$	4.20	1.360	0.759	0.583	77.25	0.758	0.585
Ti-6Al-4V	2.60	1.391	0.878	0.460	69.50	0.858	0.483
Ti-6Al-4V/TiC$_p$	2.54	1.510	1.179	0.247	52.00	1.179	0.247
Ti-6Al-4V/TiB$_w$	2.40	1.590	1.372	0.147	40.50	1.372	0.147

Strain rate sensitivity index, m =1; Die radius, a = 24 mm; Forming pressure, P = 0.2 MPa.

3.3. Instability of Deformation

Khraisheh [8] examined the failure characteristics of Pb-Sn superplastic sheet subjected to gas pressure forming. The superplastic sheet was formed using four different strain rates, and the thinning and failure characteristics in each case were observed. It was found that for low strain rate forming, failure occurred as a result of formation of tiny holes around the pole of the dome. This failure was related to the nucleation and void growth during deformation. For samples that were formed at higher strain rates, the formation of small cracks along the pole of the dome was the failure mode. It is noted that the sheet was subjected to rapid straining as well as thinning takes, just before the occurrence of the fracture near the pole of the dome. As expected the forming time for samples with slow strain rate was greater than those with higher strain rates. The forming time at failure was found to be close to the peak value of the forming pressure profile.

Table 3 gives the details on the failure pressure recorded at different strain rates. The measured limiting thickness strains in Table-3 at different applied constant strain rates are found to be almost constant. The average value of the limiting thickness strain is 1.6875.

The forming pressure at failure (P_f) in terms of the applied strain rate ($\dot{\varepsilon}_e$) is represented by [8]: $P_f = 5.5(\dot{\varepsilon}_e)^{0.25}$ MPa. Since the forming pressure in Eq. (14) is proportional to the flow stress, $\sigma\left(= K\,\dot{\varepsilon}^m\right)$, the strain rate sensitivity index (m) from the above failure pressure relation is found to be 0.25. Figures 6-9 show the comparison of the generated Pressure–time curves with the measured data [8] for m = 0.25 and 0.5. The measured pressure approaches the generated Pressure-time curve for m = 0.25 at the failure forming time.

With regard to fracture strain, the plastic behaviour of the spherical dome has to be described in terms of the local effective stress (σ_e) and the effective strain (ε_e). Since the failure occurred at the pole of the dome, the effective stress and the strain at that location are nothing but the hoop or meridional stress and the radial (thickness) strain respectively. These are to be equated to the uniaxial stress state. For the present problem, m = 0.25 and s_0 = 1.27

mm, the thickness at the pole is obtained from Eq. (12) as 0.2562 mm. From Eqs. (3) and (6), the effective strain is found as 1.601, which is close to the measured strain of 1.66 [8].

Table 3. Details on failure pressures and measured limiting thickness strains of Pb-Sn eutectic superplastically formed spherical domes at different strain rates

Strain rate $\dot{\varepsilon}_e$ (s^{-1})	Actual Failure Pressure (MPa)	Forming time to failure (seconds)	Peak Pressure P_{max} (MPa)	Measured limiting thickness strain, ε_e *	Flow Stress, $\sigma = \frac{4}{3\sqrt{3}} \frac{a}{s_0} P_{max}$ (MPa)
1 x 10^{-4}	0.512	2135	0.519	1.77	11.99
3 x 10^{-4}	0.687	935	0.691	1.66	15.96
6.5 x 10^{-4}	0.768	550	0.775	1.66	17.90
1 x 10^{-3}	1.013	195	1.039	1.66	23.99

Blank Thickness (s_0) =1.27 mm; die radius (a) = 38.1 mm.

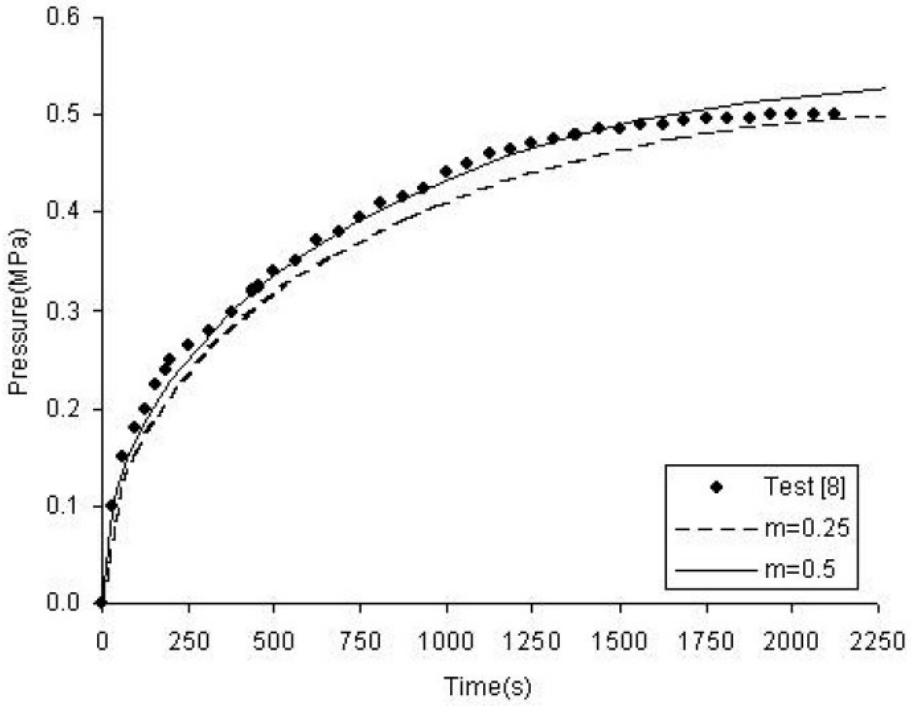

Figure 6. Forming pressure profiles of superplastic Pb-Sn eutectic alloy at strain rate=0.0001/s

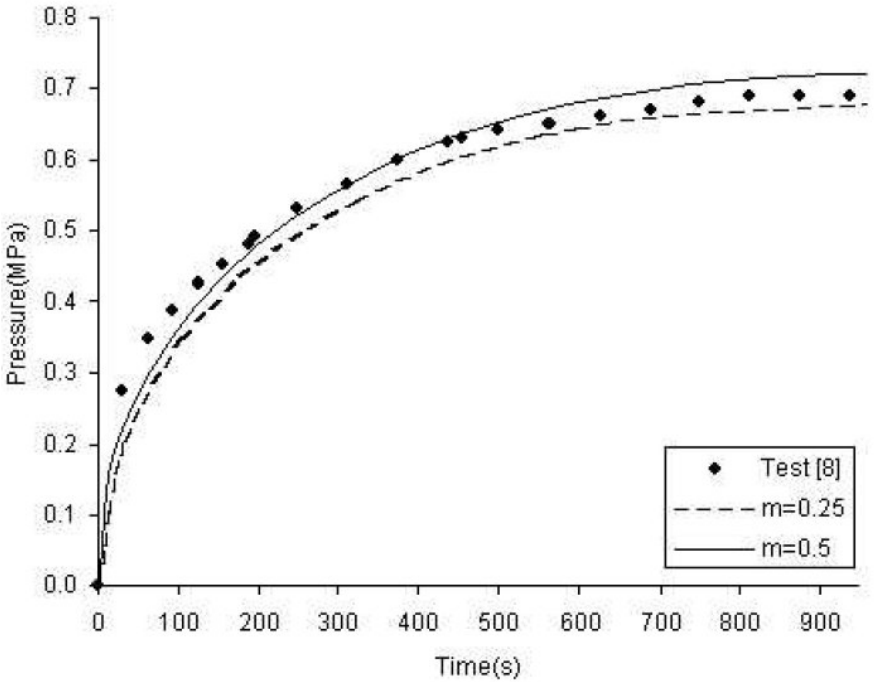

Figure 7. Forming pressure profiles of superplastic Pb-Sn eutectic alloy at strain rate=0.0003/s.

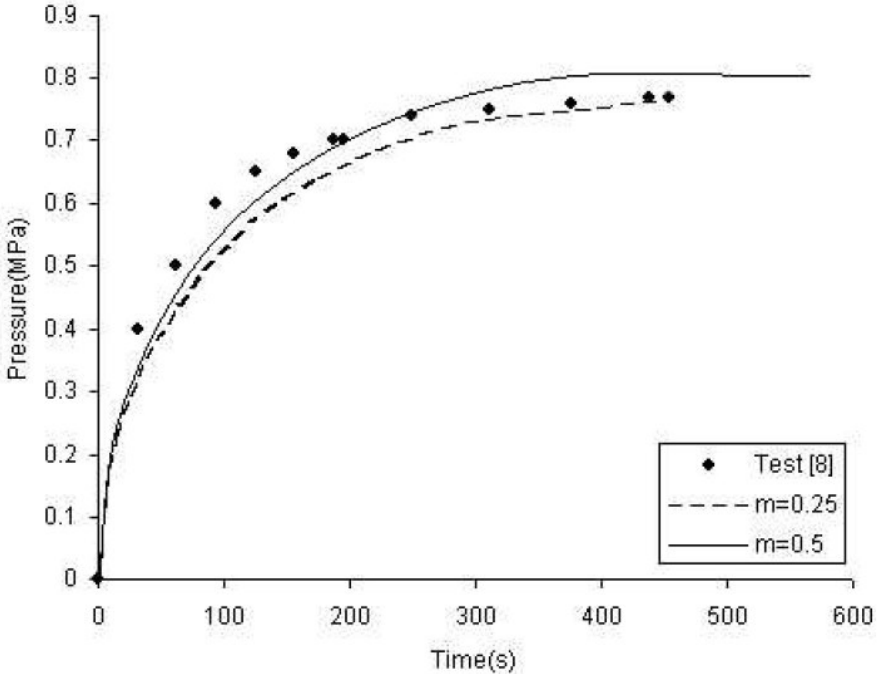

Figure 8. Forming pressure profiles of superplastic Pb-Sn eutectic alloy at strain rate=0.00065 /s.

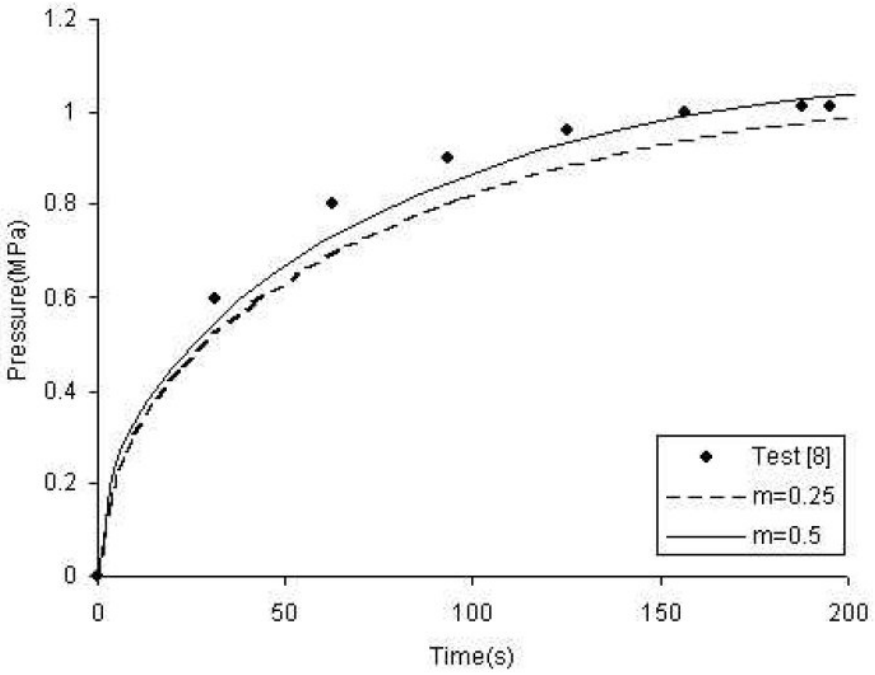

Figure 9. Forming pressure profiles of superplastic Pb-Sn eutectic alloy at strain rate=0.001/s.

A relationship for the fracture strain (e_f) derived by Ghosh and Ayres [39] is:

$$e_f = \left(1 - f^{\frac{1}{m}}\right)^{-m} - 1 \tag{24}$$

where f is the inhomogeneity factor. Woodford [40] verified the relation (24) on several materials by specifying f = 0.998 and 0.999. One of the attributes of superplastic flow that must be taken into consideration for the prediction of ductility is the case where grain coarsening is taking place [41]. In such situations, the current value of the strain rate sensitivity index (m) gradually diminishes with strain. Thus, the strain rate sensitivity index (m) can decrease from the vicinity of 0.5 to values as low as 0.25. Assuming the inhomogeneity factor, f = 0.995 as in Refs. [42], the fracture strain (e_f) from Eq. (24) for m = 0.25 is found to be 1.66414, which is in good agreement with the measured limiting thickness strains of Khraisheh [8].

CONCLUSIONS

Studies are made on the gas pressure forming of superplastic Pb-Sn eutectic alloy sheet material. A simple relation is suggested for the development of an accurate forming pressure-time curve. Expressions are provided for the thicknesses at the pole and edge of the spherical dome. The influence of strain rate sensitivity index (m) on fracture strain (e_f) is examined. The fracture occurred at the apex of domes is mainly due to low strain rate sensitivity index.

Further studies on superplastic alloys (viz., Ti, Al, Mg alloys, etc.) under multiaxial loading conditions as encountered in actual forming operations will definitely advance the utilization of SPF and improve the existing predictive capabilities.

ACKNOWLEDGEMENTS

The authors wish to thank: VSSC Editorial Board for making necessary arrangements for reviewing this article prior to its clearance for publication; Dr. P.V. Venkitakrishnan (Deputy Project Director, Materials and Hardware Production, GSLV-Mk III Projects) for his valuable comments / suggestions during the preparation of this article; Mr. G. Kothandaraman (General Manager, Mechanical Engineering Entity), Dr. P.P. Sinha (Deputy Director) for their encouragements; and Dr. B.N. Suresh, Director, VSSC for giving permission to publish this article.

REFERENCES

[1] Tsuzuku, T., Takahashi, T., Sakamoto, A., 1991. Application of superplastic forming for aerospace components. In: Hori, S., Tokizane, M., Furushiro, N. (Eds.), *Superplasticity in Advanced Materials* (ICSAM-91), JSRS, Osaka, Japan, pp.611-620.

[2] Zhang, K.F., Wang, G.F., Wu, D.Z., Wang, Z.R., 2004. Research on the controlling of the thickness distribution in superplastic forming. *J. Mater. Process. Technol*. 151, 54-57.

[3] Xing, H.L., Wang, C.W., Zhang, K.F., Wang, Z.R., 2004. Recent development in the mechanics of superplasticity and its applications. *J. Mater. Process. Technol*. 151,196-202.

[4] Chokalingam, S.K., Neelakantan, M., Devaraj, S., Padmanabhan, K.A., 1985. On the pressure forming of two superplastic alloys. *J. Mater. Sci*. 20, 1310-1320.

[5] Dutta, A., Sharma, R., 1994. Prediction of initial blank thcikness and thickness profile after superplastic forming. *Mater. Sci. Forum* 170-172, 757-762.

[6] Dunand, D.C., Myojin, S., 1997. Biaxial deformation of Ti-6Al-4V and Ti-6Al-4V/TiC composites by transformation-mismatch superplasticity. *Mater. Sci. Eng*. A 230, 25-32.

[7] Frary, M., Schuh, C., Dunand, D.C., 2002. Kinetics of biaxial dome formation by transformation superplasticity of titanium alloys and composites. *Met. Mater. Trans*. A 33, 1669-1680.

[8] Khraisheh, M.K., 2000. On the failure characteristics of superplastic sheet materials subjected to gas pressure forming. *Scripta Mater*. 42, 257-263.

[9] Wu, H.Y., 2000. Influence of strain rates and strain states on the formability of a superplastic 8090 aluminium alloy. *J. Mater. Process. Technol*. 101, 76-80.

[10] Tong, G.Q., Chan, K.C., 2002. Comparative study of a high-strain-rate superplastic Al-4.4Cu-1.5Mg / 21SiC_w sheet under uniaxial and equibiaxial tension. *Mater. Sci. Eng.* A 325, 79-86.

[11] Chan, K.C., Tong, G.Q., 2003. Formability of a high-strain rate superplastic Al-4.4Cu-1.5Mg /21SiC_w composite under biaxial tension. *Mater. Sci. Eng*. A 340, 49-57.

[12] Dutta, A., 2004. Thickness-profiling of initial blank for superplastic forming of uniformly thick domes. *Mater. Sci. Eng*. A 371, 79-81.
[13] Chung, S.W., Higashi, K., Kim, W.J., 2004. Superplastic gas pressure forming of fine-grained AZ61 magnesium alloy sheet. *Mater. Sci. Eng*. A 372, 15-20.
[14] Chan, K.C., Tong, G.Q., 2004. High-strain-rate superplastic gas pressure forming of an Al-4.4Cu-1.5Mg / 21SiC_w composite under variable strain rate paths. *Mater. Sci. Eng*. A 374, 285-291.
[15] Xing, H.L., Zhang, K.F., Wang, Z.R., 2004. A perform design method for sheet superplastic bulging with finite element modeling. *J. Mater. Process. Technol*. 151, 284-288.
[16] Yoon, J.H., Lee, H.S., Yi, Y.M., Jang, Y.S., 2007. Prediction of blow forming profile of spherical titanium tank. *J. Mater. Process. Technol*. 187-188, 463-466.
[17] Khraisheh, M.K., 2000. An investigation of yield potential in superplastic deformation, *J. Eng. Mater. Technol*. 122, 93-97.
[18] Wu, H.Y., 2000. Cavitation characteristics of a superplastic 8090Al alloy during equi-biaxial tensile deformation. *Mater. Sci. Eng*. A 291, 1-8.
[19] Lee, Y.S., Lee, S.Y., Lee, J.H., 2001. A study on the process to control the cavity and the thickness distribution of superplastically formed parts. *J. Mater. Process. Technol*. 112, 114-120.
[20] Huang, A., Lowe, A., Cardew-Hill, M.J., 2001. Experimental validation of sheet thickness optimization for superplastic forming of engineering structures. *J. Mater. Process. Technol*. 112, 136-143.
[21] Chung, L.C., Cheng, J.H., 2002. Fracture criterion and forming pressure design for superplastic bulging. *Mater. Sci. Eng*. A 333, 146-154.
[22] Aoura, Y., Ollivier, D., Ambari, A., Santo, P.D., 2004. Determination of material parameters for 7475Al alloy from bulge forming tests at constant stress. *J. Mater. Process. Technol.* 145, 352-359.
[23] Carrino, L., Giuliano, G., Ucciardello, N., 2004. Analysis of void growth in superplastic materials. *J. Mater. Process. Technol*. 155-156, 1273-1279.
[24] Kalaichelvan, K., Sivaramakrishnan, R., Dinakaran, D., Stanley, A.J., 2007. Cavity minimization and uniformity studies on superplastic forming of thin eutectic Pb-Sn sheet by optimum loading and performing. *J. Mater. Process. Technol*. 191, 189-192.
[25] Senthil Kumar, V.S., Viswanathan, D., Natarajan, S., 2006. Theoretical prediction and FEM analysis of superplastic forming of AA7475 aluminium alloy in a hemispherical die. *J. Mater. Process. Technol*. 173, 247-251.
[26] Giuliano, G., Carrino, L., Franehitti, S., 2006. Modeling the free forming of superplastic Pb-Sn60 at constant pressure. *J. Mater. Process. Technol*. 177, 95-97.
[27] Nazzal, M.A., Khraisheh, M.K., Abu-Farha, F.K., 2007. The effect of strain rate sensitivity evolution on deformation stability during superplastic forming. *J. Mater. Process. Technol*. 191, 189-192.
[28] Luckey Jr., S.G., Friedman, P.A., Weinmann, K.J., 2007. Correlation of finite element analysis to superplastic forming experiments. *J. Mater. Process. Technol*. 194, 30-37.
[29] Dutta, A., Mukherjee, A.K., 1992. Superplastic Forming: an analytical approach. *Mater. Sci. Eng*. A 157, 9-13.
[30] Enikeev, F.U., 1994. An analytical model for superplastic bulge forming of domes. *Mater. Sci. Forum* 170-172, 681-686.

[31] Cheng, J.H., 1996. The determination of material parameters from superplastic inflation tests. *J. Mater. Process. Technol*. 58, 233-246.

[32] Jeyasingh, J.J.V., Dhananjayan, K., Sinha, P.P., Nageswara Rao, B., 2004. Prediction of non-uniform thinning in superplastically formed spherical domes. *Mater. Sci. Technol*. 20, 229-234.

[33] Jeyasingh, J.J.V., Nageswara Rao, B., 2005. On the thinning variation of a superplastically formed titanium alloy spherical domes. *J. Mater. Process. Technol*. 160, 370-373.

[34] Geckinli, A.E., Barrett, C.R., 1976. Superplastic deformation of the Pb-Sn eutectic. *J. Mater. Sci.* 11, 510-521.

[35] Hamilton, C.H., Zhang, K., Khraisheh, M., Zbib, H.M., 1995. Superplastic flow under transient conditions and multiaxial stresses. In: Ghosh, A.K., Bieler, T.R. (Eds.), *Superplasticity and Superplastic Forming, The Minerals, Metals and Materials Society*, Warrendale, PA, pp.181-188.

[36] Jeyasingh, J.J.V., Nageswara Rao, B., 2005. Failure analysis on gas pressure formed spherical domes of Pb-Sn eutectic alloy. *Mater. Sci. Technol*. 21, 1359-1362.

[37] Jeyasingh, J.J.V., Dhananjayan, K., Kothandaraman, G., Sinha, P.P., Nageswara Rao, B., Chennakesava Reddy, A., 2005. Studies on the gas pressure formed Pb-Sn eutectic alloy spherical domes. In: Kothandaraman, G. (Chairman), *Proc. Second National Seminar on Aerospace Manufacturing Future Trends, Organized by Society of Aerospace Manufacturing Engineers (SAME)*, Trivandrum, India (NAMS-2005), pp. 268-276.

[38] Chandra, N., 2002. Constitutive behaviour of superplastic materials. I*nt. J. Non-Linear Mech.* 37, 461-484.

[39] Ghosh, A.K., Ayres, R.A., 1976. On reported anomalies in relating strain rate-sensitivity (m) to ductility. *Met. Trans.* A 7, 1589-1591.

[40] Woodford, D.A., 1969. Strain-rate sensitivity as a measure of ductility. *Trans. ASM 62*, 291-293.

[41] Jonas, J.J., 1982. Implications of flow hardening and flow softening during superplastic forming. In: Paton, N.E., Hamilton, C.H. (Eds.), *Superplastic Forming of Structural Alloys,* The Metallurgical Society of AMIE, Warrendale, PA, pp.57-68.

[42] Lian, J., Baudelet, B., 1986. Necking development and strain to fracture under uniaxial tension. *Mater. Sci. Eng*. A 84, 157-162.

Reviewed by
Dr. P.V. Venkitakrishnan
Deputy Project Director, Materials and Hardware Production
GSLV-Mk III Projects
Vikram Sarabhai Space Centre, Trivandrum – 695 022, India